⌘ *Author's Choice*

THE JOURNAL OF BIOLOGICAL CHEMISTRY VOL. 287, NO. 22, pp. 18005–18017, May 25, 2012

Transglutaminase-2 Interaction with Heparin

IDENTIFICATION OF A HEPARIN BINDING SITE THAT REGULATES CELL ADHESION TO FIBRONECTIN-TRANSGLUTAMINASE-2 MATRIX[*S]

Received for publication, December 22, 2011, and in revised form, February 24, 2012 Published, JBC Papers in Press, March 22, 2012, DOI 10.1074/jbc.M111.337089

Hugues Lortat-Jacob[‡1,2], Izhar Burhan[§1], Alessandra Scarpellini[§], Aline Thomas[¶], Anne Imberty[¶], Romain R. Vivès[‡], Timothy Johnson[‖], Aldo Gutierrez[§], and Elisabetta A. M. Verderio[§2]

From the [‡]CNRS- Commissariat à l'Energie Atomique-Université Joseph Fourier, Grenoble 1, Institut de Biologie Structurale Jean-Pierre Ebel, 38027, Grenoble cedex 01, France, [§]School of Science and Technology, Nottingham Trent University, Nottingham NG11 8NS, United Kingdom, [¶]Centre de Recherches sur les Macromolécules Végétales-CNRS, 38041 Grenoble cedex 9, France, and [‖]Academic Nephrology Unit, University of Sheffield, Sheffield S10 2RZ, United Kingdom

Background: Extracellular transglutaminase-2 binds heparan sulfate and has adhesive/signaling pro-fibrotic functions.
Results: Two clusters of basic residues, distal in the linear sequence of transglutaminase-2, are required for heparin binding and cell adhesion.
Conclusion: Folding of the transglutaminase-2 protein brings basic residues in close proximity to form a functional heparin binding domain.
Significance: Mapping the heparan sulfate binding domain will enhance design of transglutaminase-2 inhibitors.

Heparan sulfate proteoglycans are critical binding partners for extracellular tranglutaminase-2 (TG2), a multifunctional protein involved in tissue remodeling events related to organ fibrosis and cancer progression. We previously showed that TG2 has a strong affinity for heparan sulfate (HS)/heparin and reported that the heparan sulfate proteoglycan syndecan-4 acts as a receptor for TG2 via its HS chains in two ways: by increasing TG2-cell surface trafficking/externalization and by mediating RGD-independent cell adhesion to fibronectin-TG2 matrix during wound healing. Here we have investigated the molecular basis of this interaction. Site-directed mutagenesis revealed that either mutation of basic RRWK (262–265) or KQKRK (598–602) clusters, forming accessible heparin binding sequences on the TG2 three-dimensional structure, led to an almost complete reduction of heparin binding, indicating that both clusters contribute to form a single binding surface. Mutation of residues Arg^{19} and Arg^{28} also led to a significant reduction in heparin binding, suggesting their involvement. Our findings indicate that the heparin binding sites on TG2 mainly comprise two clusters of basic amino acids, which are distant in the linear sequence but brought into spatial proximity in the folded "closed" protein, forming a high affinity heparin binding site. Molecular modeling showed that the identified site can make contact with a single heparin-derived pentasaccharide. The TG2-heparin binding mutants supported only weak RGD-independent cell adhesion compared with wild type TG2 or mutants with retained heparin binding, and both heparin binding clusters were critical for TG2-mediated cell adhesion. These findings significantly advance our knowledge of how HS/heparin influences the adhesive function of TG2.

Transglutaminase type 2 (TG2)[3] (EC 2.3.2.13) belongs to an emerging category of proteins with distinct molecular activities that function both inside and outside the cell and transit the plasma membrane by unconventional secretion (1, 2). Outside the cell TG2 regulates the extracellular matrix (ECM) organization and modulates cell-ECM adhesion and outside-in signaling (3), whereas in the intracellular environment TG2 participates into signaling events leading to regulation of cell survival, particularly in response to cell wounding, hypoxia, and oxidative stress (4–6). TG2 is ubiquitously expressed and plays a pleiotropic role in a variety of pathophysiological conditions related to tissue remodeling including cancer development, organ fibrosis, and neurodegeneration (7–11). Protein transamidation, leading to ϵ(γ-glutamyl)lysine intra- or intermolecular isopeptide bonds ("protein cross-links"), is the enzymatic reaction for which TG2 is better recognized, which is regulated by Ca^{2+} binding and guanine nucleotide dissociation, a condition favored in the extracellular environment or after cell injury and loss of Ca^{2+} homeostasis (12). Furthermore, TG2-mediated protein deamidation of Gln residues contributes to the adaptive immunoresponse induced in gluten sensitivity diseases (13). In the intracellular environment TG2 can serve as a an unconventional GTPase whose GTP binding and hydrolysis site is integrated with the Ca^{2+}-regulated transamidase active site (14, 15). In the ECM the role of TG2 is largely linked to its interaction with fibronectin, which occurs via the N-terminal β-sand-

* This work was supported in part by Wellcome Trust Project 087163 (to E. A. M. V. and T. J.) and by Nottingham Trent University-RAE QR (U12) fund (to E. A. M. V. and A. G.).
⌘ *Author's Choice*—Final version full access.
[S] This article contains supplemental Table 1 and Figs. 1–3.
[1] Both authors contributed equally to this work.
[2] To whom correspondence may be addressed: School of Science and Technology, Biomedical Life and Health Science Research Centre, Nottingham Trent University, Nottingham NG11 8NS, UK. Tel.: 44-115-848-6628; Fax: 44-115-848-6636; E-mail: elisabetta.verderio-edwards@ntu.ac.uk or CNRS-CEA-UJF-Grenoble 1, Institut de Biologie Structurale Jean-Pierre Ebel, 41 rue Horowitz, 38027, Grenoble cedex 01, France. Tel.: 33-438-784-485; Fax: 33-438-785-494; E-mail: hugues.lortat-jacob@ibs.fr.

[3] The abbreviations used are: TG2, transglutaminase-2; sdc-4, syndecan-4; HS, heparan sulfate; ECM, extracellular matrix; Boc-DON, Boc-DON-Gln-Ile-Val-OMe; FN, fibronectin.

wich domain of TG2, leading to cell-matrix adhesion, cell migration, and signaling (3, 12, 16, 17). The extracellular function of TG2 only partly depends on protein cross-linking (*e.g.* leading to fibronectin remodeling). TG2 supports adhesion-mediated cell signaling through a well described non-enzymatic function by acting as a cell surface integrin-β1 co-receptor for fibronectin (18) or by ligating syndecan-4 (sdc-4) receptor once deposited in the ECM in a TG2-fibronectin heterocomplex (19, 20).

TG2 contributes to the regulation of extracellular and intracellular events. However, how TG2 dual location may be coordinated to allow for flexibility of localization/function and how the balance between catalytically active and inactive TG2 is maintained in the extracellular environment remains to be clarified (21). It has been recently proposed that TG2 is externalized via recycling endosomes in which it is delivered by binding to phospholipids and an unknown endosomal receptor(s), based on a model of fibroblasts expressing exogenous TG2 (22). In our laboratory we previously identified a strong affinity of TG2 for heparan sulfate (HS) glycosoaminoglycans and its association with the aforementioned HS proteoglycan receptor sdc-4. We demonstrated that the HS chains of sdc-4 have a dual role in regulating TG2 function; that is, by controlling the cell surface trafficking/ECM distribution of TG2 *in vitro* and *in vivo* during experimental kidney fibrosis (23, 24) and by mediating RGD-independent cell adhesion induced by matrix TG2 in heterocomplex with fibronectin (19, 20, 25). This alternative cell adhesion pathway complements the classic integrin-dependent RGD pathway, leading to RGD-independent activation of protein kinase Cα, focal adhesion kinase, and ERK1/2 protein kinases (20). This process is particularly relevant in situations of cell damage/matrix fragmentation and increased deposition of TG2 in the matrix once integrin-mediated signaling is compromised (3).

Heparan sulfate (26) glycosoaminoglycans are well recognized regulators of cell functions by acting as signaling co-receptors, modulators of tissue distribution, and cellular trafficking for a variety of molecules. HS is a complex polysaccharide consisting of disaccharide units and is linked to specific cell surface proteins (*e.g.* the aforementioned syndecans and glypicans) and ECM proteins (agrin, perlecan, collagen XVIII). The HS chains consist of alternating *N*-acetylated or *N*-sulfated glucosamine units (GlcNAc or *N*-sulfoglucosamine) and uronic acids (glucuronic acid or iduronic acid). The assembly of HS chains on core proteins is characterized by great variability and processing reactions (GlcNac *N*-deacetylation, *N*-sulfation, epimerization, and *O*-sulfation), which progress at different extents to generate patterns of highly negatively charged binding sites responsible for binding to a variety of protein ligands (among which fibroblast growth factor (FGF)/FGF receptor is well documented (27)).

Although the crystallographic structure of TG2 has been defined (28, 29), the heparin binding site in TG2 has not been determined. Given the potential key role of HS proteoglycans in controlling the trafficking and the extracellular adhesive functions of TG2 *in vitro* and *in vivo*, we have begun investigating the nature of this interaction. In this study we have mapped a high affinity heparin binding site on TG2 and showed that it comprises two distant clusters of basic amino acids that are brought into close proximity on the folded protein. We have also shown that the identified heparin binding site is critical for cell adhesion to TG2-fibronectin matrix. These data significantly advance our knowledge of how HS/heparin interacts with and influences the adhesive function of TG2.

EXPERIMENTAL PROCEDURES

Protein Expression, Purification, and Analysis—Human TG2 cDNA (30) was subcloned into pET21a(+) (Novagen) between NheI and HindIII restriction enzyme sites (pET21a(+)TG2). Using *pET21a(+)TG2* as reaction template, mutants of residues predicted to be involved in heparin binding were produced by QuikChange II site-directed mutagenesis (Stratagene) using *PfuUltra* high fidelity DNA polymerase and mutagenic oligonucleotide primers (Sigma Genosys) (supplemental Table 1). Single or multiple amino acids residues were substituted to serine as summarized in Table 1. The point mutations were confirmed by sequencing using standard T7-Promoter Primer or T7-Terminator Primer (SourceBioscience). To produce TG2 protein, pET21a(+)TG2 was expressed in BL21 (DE3) cells (Novagen). After cell growth in Luria Bertani medium containing ampicillin (100 μg/ml) (up to A_{600} 0.6), expression of recombinant His-tagged TG2 was induced by the addition of isopropyl 1-thio-β-D-galactopyranoside (1 μM) and incubation at 20 h at 20 °C as described (31). Mutant (M) TG2 constructs were expressed and purified using the same protocol except for M1a, M1b, and M1c whose expression was induced by 100 μM isopropyl 1-thio-β-D-galactopyranoside. After induction, cells were recovered by centrifugation (4000 $\times$ *g* at 4 °C for 30 min). The pellet was resuspended in lysis buffer (50 mM Na_3PO_4 (pH 8.0), 300 mM NaCl) supplemented with 10 mM imidazole and 1 mM EDTA, lysed by sonication (Soniprep) for 60 s (amplitude 12), and incubated with 2 mg/ml lysozyme on ice for 30 min (Sigma) followed by 3 more rounds of sonication. After centrifugation (40,000 $\times$ *g* at 4 °C for 45 min), the supernatant was applied to a column holding 15 ml of Ni-His60 Superflow resin (Clontech). The column was washed once with lysis buffer containing, first, 10 mM imidazole and then 40 mM imidazole until no proteins were detected in the wash buffer (as monitored by the UV flow cell of Biologic HR chromatography (Bio-Rad)). TG2 was eluted in buffer containing 400 mM imidazole. Fractions containing TG2 (as monitored by SDS-PAGE) were pooled and exchanged in 50 mM Tris-HCl (pH 8.0), 50 mM NaCl, 2 mM DTT and 1 mM EDTA. They were then further purified on a Hi-Trap HP column (GE Healthcare) employing a gradient of NaCl (0–1 M) in 50 mM Tris-Cl (pH 8.0), 2 mM DTT, and 1 mM EDTA. Recombinant TG2 was eluted between at 330–440 mM NaCl, concentrated using VivaSpin 30,000 M_r cutoff concentrator (Vivabioscience) and exchanged in 50 mM Na_3PO_4 (pH 8.0), 150 mM NaCl, 2 mM DTT, 1 mM EDTA. After the addition of maltodextrin to the concentration of 5% (w/v), the protein was stored at −80 °C. Proteins were analyzed by 10% (w/v) acrylamide gels for SDS-PAGE followed by Instant Blue staining (Expedeon) and Western blotting as previously described (23) using horseradish peroxidase-conjugated mouse anti-His6 antibody (Roche Applied Science).

Thermal Shift Assay—Thermal shift assay analyses were performed using a IQ5 real-time PCR system as previously described (32). Briefly, wild type (wt) or mutant TG2 (23 μl at 0.5 mg/ml) were mixed with 2 μl of a 100× SYPRO Orange solution in water (Molecular Probes, Invitrogen). Samples were heated from 20 to 100 °C at 1 °C/min rate. Protein unfolding was followed by fluorescence measurement (excitation/emission 583/610 nm) every 0.2 s. Melting temperature (Tm) was determined for each sample by analyzing the collected data with a custom differential scanning fluorimetry analysis software as described before (33).

TG2 Activity Assay—TG2 activity was measured by the incorporation of biotinylated cadaverin into fibronectin as described previously (34). Briefly, recombinant and mutant TG2 (100 ng) were incubated in fibronectin-coated 96-well plates in reaction buffer (50 mM Tris-HCl (pH 7.4), 5 mM $CaCl_2$, 10 mM DTT, and 0.1 mM biotinylated cadaverine) in a final volume of 100 μl for 2 h at 37 °C. Background TG2 activity values were obtained by replacing 5 mM $CaCl_2$ with 5 mM EDTA in the reaction buffer. The reaction was stopped by the addition of PBS (pH 7.4) containing 10 mM EDTA. The level of incorporated biotin-cadaverine into fibronectin was revealed by incubation with extravidin peroxidase followed by the addition of 3,3′,5,5′-tetramethylbenzidine at fixed times and stopped by 0.5 M H_2SO_4. Spectrophotometric absorbances were measured at 450 nm. Background TG2 activity values in the presence of EDTA were subtracted from activity values at 5 mM Ca^{2+}. Calibration curves were obtained with known units of commercial recombinant TG2 (Sigma). Ca^{2+}activation of wt and mutant TG2 was determined at increasing concentrations of added Ca^{2+} (0–5 mM). Guanosine-5′-triphosphate (GTP) inhibition was assayed at increasing GTP concentrations (0–2 mM) in the presence of a fixed concentration of Ca^{2+} (150 μM).

Stabilization of TG2 into "Open" Conformation—TG2 was incubated with active-site directed inhibitors R283 (1,3-dimethyl-2-[(2-oxopropyl)thio]imidazolium chloride) (30 μM) or Boc-Don (Boc-DON-Gln-Ile-Val-OMe) (3 μM), both from Zedira GmbH, in the presence of 10 mM $CaCl_2$ for 5 min at 37 °C according to the manufacturer's instructions. Commercial open His-TG2 (Open tTG™, Zedira GmbH), produced in insect cells and stabilized in the open conformation via the peptidomimetic blocker ZED754 by the manufacturer, was also utilized.

Biotinylation Procedure and Heparin Immobilization—Heparin (6 kDa) (Sigma) was biotinylated at the reducing end (Biotin-LC-hydrazide, Pierce) as described previously (38) and immobilized on a CM4 Biacore sensorchip (GE Healthcare) using an amine coupling kit. Briefly, a Biacore 3000 system (GE Healthcare) was equilibrated with running buffer HBS-EP (10 mM HEPES, 150 mM NaCl, 3 mM EDTA, 0.05% surfactant P20, pH 7.4) at 5 μl/min, and the temperature was maintained at 25 °C. Two flow cells of a CM4 sensorchip were activated with 50 μl of a mixture of 0.2 M l-ethyl-3-(3-dimethylaminopropyl) carbodiimide, 0.05 M *N*-hydroxysuccinimide before injection of 50 μl of streptavidin (0.1 mg/ml in 10 mM acetate buffer (pH 4.2)). Remaining activated groups were blocked with 50 μl of ethanolamine 1 M, pH 8.5. Typically, this procedure allowed coupling of approximately ~ 2500 resonance units of streptavidin. Biotinylated heparin (5 μg/ml in HBS-EP containing 0.3 M NaCl) was then injected on one of the two streptavidin surface (the other one being a negative control) until an immobilization level of 50 resonance units was achieved. Both flow cells were then conditioned with several injections of 1 min of 0.1% SDS and 4 min of 2 M NaCl.

TG2/Heparin Interaction—For binding assays, test samples (wt or mutant TG2) were diluted in HBS-EP buffer maintained at 25 °C and injected over both a reference and the heparin surfaces at a flow rate of 20 μl/min for 5 min after which the formed complex was washed with another 5 min of running buffer. The sensorchip surfaces were regenerated with a 1-min pulse of 0.1% SDS and a 4-min pulse of 2 M NaCl. In a typical analysis, six different TG2 concentrations were injected. Apparent dissociation constants (K_D) were estimated by fitting the steady state values at equilibrium (R_{eq}) assuming one binding site with $R_{eq} = R\max_{eq}/(K_D + c)$ and by plotting (R_{eq}) divided by the concentrations of injected TG2 (c) against the R_{eq} for different concentrations of the protein (Scatchard analysis).

Molecular Modeling—Among the three available crystal structures of human TG2 (28, 29), the structure of the complex with ATP solved at 3.1 Å (PDB code 3LY6) (29) was selected for the modeling study. It corresponds to a closed conformation, and very few residues are missing in the structures. The residues identified by mutagenesis studies as interacting with heparin were graphically analyzed, with special attention for residues Arg^{28}, Arg^{262}, Arg^{263}, Lys^{265}, Arg^{598}, Lys^{600}, Lys^{602}, and Lys^{634}. When necessary, the orientations of the side chains of these amino acids were modified to point toward the solvent and interact favorably with negatively charged ligands. The orientation of the side chain of Glu^{632} was also modified to break the salt chain with Lys^{634}, which then could act as possible ligand binding residue. All calculations were performed using the Schrödinger suite. The OPLS-2005 force-field (35) was used for the protein preparation, and the residues charges were assigned considering a pH of 7.0. The receptor model was subjected to a short energy minimization procedure of 100 steps of conjugate gradient using the Impact facility of the Schrödinger Suite with a dielectric constant of 1, a residue-based non-bonded cut-off of 12 Å, and a 10-step interval for update of the non-bonded list.

For the docking calculations, a pentasaccharide of heparin with Ido2s at reducing and non-reducing ends was extracted from the PDB structure 1HPN (36) with iduronic ring in $^1C_4$ conformation. A preliminary conformational search was performed on the pentasaccharide using the module Macromodel of the Schrödinger Suite 2010 (MacroModel 9.1, Schrödinger, Inc., L.L.C., New York, NY) while constraining the conformation of all rings. A set of 16 low energy conformers was obtained and submitted to a docking calculation using Glide version 5.6 (Schrödinger Suite 2010) (37). The box used for the docking studies was generated from a manual docking of a hexasaccharide in the vicinity of the residues characterized from mutagenesis studies. A flexible docking in standard precision was performed allowing sampling of the nitrogen inversions but not of the ring conformations. For each of the 16 conformers, 5000 initial poses were selected, and the best 400 poses were sub-

A

MAEELVLE**R**CDLELETNG**R**DHHTADLC**R**E**K**LVV**RR**GQPFWLTLHFEG**R**NYEASVD
SLTFSVVTGPAPSQEAGT**K**A**R**FPL**R**DAVEEGDWTATVVDQQDCTLSLQLTTPANAPI
GLY**R**LSLEASTGYQGSSFVLGHFILLFNAWCPADAVYLDSEEE**R**QEYVLTQQGFIYQ
GSA**K**FI**K**NIPWNFGQFEDGILDICLILLDVNP**K**FL**K**NAG**R**DCS**RR**SSPVYVG**R**VGSGM
VNCNDDQGVLLG**R**WDNNYGDGVSPMSWIGSVDIL**RR**W**K**NHGCQ**R**V**K**YGQCWVF
AAVACTVL**R**CLGIPT**R**VVTNYNSAHDQNSNLLIEYF**R**NEFGEIQGD**K**SEMIWNFHCW
VESWMT**R**PDLQPGYEGWQALDPTPQE**K**SEGTYCCGPVPV**R**AI**K**EGDLST**K**YDAPFV
FAEVNADVVDWIQQDDGSVH**K**SIN**R**SLIVGL**K**IST**K**SVG**R**DE**R**EDITHTY**K**YPEGSSE
E**R**EAFT**R**ANHLN**K**LAE**K**EETGMAM**R**I**R**VGQSMNMGSDFDVFAHITNNTAEEYVC**R**
LLLCA**R**TVSYNGILGPECGT**K**YLLNLNLEPFSE**K**SVPLCILYE**K**Y**R**DCLTESNLI**K**V**R**
ALLVEPVINSYLLAE**R**DLYLENPEI**K**I**R**ILGEP**K**Q**K**R**K**LVAEVSLQNPLPVALEGCTFT
VEGAGLTEEQ**K**TVEIPDPVEAGEEV**K**V**R**MDLLPLHMGLH**K**LVVNFESD**K**L**K**AV**K**G
F**R**NVIIGPALEH

B

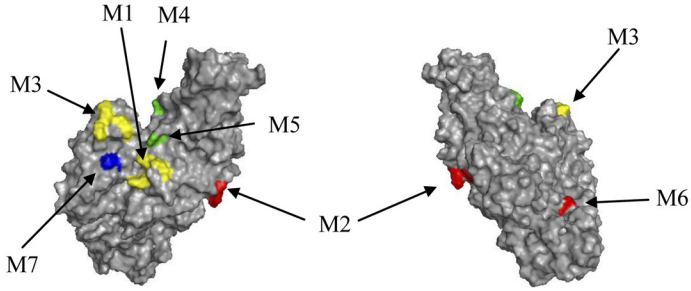

FIGURE 1. **Identification of potential heparin binding sites on the TG2 sequence.** *A*, shown is the amino acid sequence of TG2. The basic residues Arg and Lys are in *bold*, and the *colored boxes* indicate residues investigated by mutagenesis. *B*, the structure of TG2 (PDB code 3LY6) shows the surface localization of residues corresponding to TG2 mutants M1 and M3 (*yellow*), M2 and M6 (*red*), M4 and M5 (*green*), and M7 (*blue*). The drawings were prepared with PyMOL.

jected to post-docking minimization using 100 steps of conjugate gradient. The ligand poses were ranked according to their Glide scores.

Assay of RGD-independent Cell Adhesion to TG2-Fibronectin Matrix—The adhesion of Swiss 3T3 albino fibroblasts to TG2-fibronectin was assayed as described before (19). Briefly, fibronectin matrix (5 μg/ml) was immobilized on tissue culture plastic (wells of 96-well plates), blocked in 3% (w/v) lipid-free milk protein (Marvel), and supplemented with TG2 protein (20 μg/ml) in the presence of 2 mM EDTA. To measure RGD-independent cell adhesion, exponentially growing cells were preincubated with GRGDTP synthetic peptide (100 μg/ml) or similar concentrations of control inactive GRADSP peptide (Merck) in suspension in serum-free Dulbecco's modified Eagle's medium (DMEM) before being seeded on fibronectin matrix alone or in complex with TG2. After 20 min of cell adhesion, the adhered cells were stained with May Grünwald and Giemsa stain (Sigma) and assessed in terms of cell attachment and cell spreading as described previously (23) using ImageJ (9 images/well). The presence of wt and mutant TG2 immobilized on fibronectin was confirmed by an ELISA-type assay using HRP-conjugated anti-His6 antibody (Roche Applied Science) as previously described (19).

Statistics—Statistical significance was tested by one-way analysis of variance using Dunnett's post-test (EC_{50} for Ca^{2+} and IC_{50} for GTP) or Bonferroni's post-test (cell adhesion assay); *, $p < 0.05$; **, $p < 0.01$; ***, $p < 0.001$.

RESULTS

Identification of Potential Heparin Binding Sites—Identification of heparin binding sites on proteins remains a complex issue. Early work, based on heparin binding protein sequence comparison, led to the proposition of two binding consensus sequences, *X*BB*X*B*X* and *X*BBB*XX*B*X*, where B stands for a basic, and X is for a neutral/hydrophobic amino acid (38). This, however, does not exclude that patterns of positively charged residues comprise distant amino acids clustered by the protein folding (39). Examination of the TG2 sequence (Fig. 1*A*) reveals the presence of several basic residues (38 Arg and 32 Lys residues), some of which are organized into two typical heparin binding site, *i.e.* RRWK and KQKRK (positions 262–265 and 598–602, respectively). Analysis of the three-dimensional structure of the protein (Fig. 1*B*) showed that these two clusters, although distant on the protein sequence, are close to each other on the TG2 surface. Further examination of the protein structure also revealed that three basic residues, Arg^{19} and Arg^{28} and Lys^{634} are in close proximity of these two clusters. Thus, based on this analysis, TG2 mutants targeting these domains were produced as well as two further residues, Lys^{202} and Lys^{205}, which form a well exposed positively charged cluster on the opposite face of the protein, and Arg^{580} in the GTP binding pocket.

Production and Purification of Recombinant wt and Mutant TG2—Full-length human TG2 was expressed and purified by using a modified version of the two-step purification process developed by Piper *et al.* (31). Thirteen sequence positions of TG2 (30) were selected for mutagenesis (Arg^{19}; Arg^{28}; Lys^{202}/Lys^{205}; Arg^{262}; Arg^{263}; Lys^{265}; Arg^{580}; Lys^{598}/Lys^{600}/Arg^{601}/Lys^{602}; Lys^{634}), and a total of nine single and multiple site mutant constructs were generated where the basic residues (Arg, Lys) were replaced by Ser (which better maintains a certain level of hydrophilicity than the Ala residue). All the TG2 mutants were expressed at milligram levels with purity similar

TABLE 1

Calcium activation and GTP inhibition of transglutaminase activity

The activity of transglutaminase was determined at increasing concentrations of Ca^{2+} or GTP as described under "Experimental Procedures." Activities are reported as the percentage of maximal activity. EC_{50} for Ca^{2+} activation (Fig. 2*A*) and IC_{50} for GTP inhibition (Fig. 2*B*) were estimated using GraphPad Prism. TG specific activity values at the plateau Ca^{2+} level (5 mM) are also shown. All values are expressed as the means S.E. for at least 3 independent experiments. Significant differences between wt and mutant TG2 are shown.

Protein	Substitution	EC_{50} (Ca^{2+})	IC_{50} (GTP)	TG specific activity
		μM	μM	*Units/mg*
TG2	wt	86 ± 9	142 ± 24	3.9 ± 0.4
M1a	R262S	258 ± 32[a]	23 ± 5[b]	2.8 ± 0.3
M1b	R263S	195 ± 56[b]	79 ± 15	2.7 ± 0.1[b]
M1c	K265S	123 ± 13	182 ± 17	3.1 ± 0.1
M2	K202S/K205S	68 ± 4	145 ± 23	3.8 ± 0.3
M3	K598S/K600S/R601S/K602S	136 ± 13	148 ± 26	3.6 ± 0.2
M4	R19S	67 ± 7	254 ± 8[b]	3.7 ± 0.5
M5	R28S	115 ± 17	64 ± 27	3.4 ± 0.2
M6	R580S	64 ± 3	No inhibition	4.8 ± 0.4
M7	K634S	260 ± 30[a]	199 ± 36	3.2 ± 0.2

[a] $p < 0.001$.
[b] $p < 0.05$.

to wt TG2 (supplemental Fig. 1). To test whether the TG2 mutants retained the typical transamidating activity of TG2, which is dependent on Ca^{2+} and regulated by guanine nucleotides, we measured the Ca^{2+} requirement for the mutants compared with wt TG2. Dose-response curves for Ca^{2+} activation were obtained by increasing the concentration of added Ca^{2+} (0–5 mM) (Fig. 2*A*). All the TG2 mutants showed Ca^{2+} dependence. Wt TG2 reached half-maximal activation at ~90 μM Ca^{2+} concentration (Table 1). There were no significant differences in EC_{50} for Ca^{2+} activation between wt TG2 and the mutants except for M1a (Arg^{262}), M1b (Arg^{263}), and M7 (Lys^{634}), which reached ~30–40% activity at the EC_{50} (Ca^{2+}) of wt TG2. However, only M1b displayed a significantly lower level of specific activity than the wt enzyme at saturating levels of Ca^{2+} (Table 1). The GTP inhibition of wt and mutant TG2 was evaluated in the presence of 150 μM Ca^{2+} (which corresponds to ~70% of maximum activity of wt TG2). GTP was capable of inhibiting all the mutant enzymes similarly to wt TG2 (Fig. 2*B*), with only M1a (Arg^{262}) and M4 (Arg-19) being slightly more and less sensitive, respectively, to GTP inhibition (Table 1). Mutant M6, corresponding to the GTP binding residue Arg^{580}, was found not to be GTP-dependent, as previously shown (40). All together these results indicate that all the TG2 mutants, except for the GTP binding mutant M6, retained the ability to be modulated by Ca^{2+} and GTP as wt TG2. It can be concluded that all these mutations do not disrupt the bifunctional property of TG2, indicating that the proteins were properly folded. Thermal shift analysis showed that the TG2 mutants had very similar stability to wt TG2, a finding that is consistent with their correct folding (supplemental Fig. 2). Therefore, the TG2 mutants were next investigated for their heparin binding properties.

Experimental Identification of TG2 Amino Acids Involved in Heparin Binding—The binding properties of the wt and mutated recombinant TG2 were tested using a solid phase assay in which biotinylated heparin was immobilized on top of a streptavidin-coated sensorchip. This system mimicked to some extent the cell membrane-anchored proteoglycan, and surface plasmon resonance spectroscopy was used to measure changes in the refractive index caused by the interaction that occurred when TG2 was flowed across the immobilized heparin surface. Dose-response experiments were performed with the wt TG2 injected in the 66–500 nM range. The association phase (from 100 to 400 s) was allowed to proceed to equilibrium (Fig. 3*A*), and affinity data were derived as described under "Experimental Procedures." This returned an affinity of K_D = 181 nM. As heparin is heterogeneous in sequence and is thus likely to display different binding sites, the above calculated value should be regarded as an "average affinity" constant. Nevertheless, this indicated a relatively strong affinity between TG2 and heparin. Next, the same assay was used to determine the binding strength of the different TG2 mutants. Each of the residues of the first BBXB cluster (Arg^{262}, Arg^{263}, and Lys^{265}) was found critically important for heparin recognition, as none of the corresponding mutants (M1a, M1b, and M1c) strongly bound to the immobilized glycosoaminoglycan (Fig. 3, *B–D*). Similarly, the mutant corresponding to the second cluster (M3; KQKRK) was strongly impaired in its ability to bind heparin (Fig. 3*E*). Then, to investigate whether residues Arg^{19} and Arg^{28}, both located close to the above-analyzed residues, could be part of the binding site, the TG2 mutants (M4 and M5) corresponding to these two residues were injected over the heparin surface. Although these mutants still interacted with heparin, they both displayed defects in heparin binding (Fig. 3, *F* and *G*). The TG2 mutant M7, corresponding to residue Lys^{634}, bound very well to heparin but at a much lower rate, as equilibrium was not reached after the 5-min association phase, compared with wt TG2 (Fig. 3*H*), supporting its involvement in heparin recognition. Finally, we also analyzed the effect of two additional mutants, the M2 mutant (Lys^{202}, Lys^{205}) whose mutated residues are located on the opposite face of the protein, and the M6 mutant (Arg^{580}). Both displayed strong binding (Fig. 3, *I* and *J*), returning affinity values of 162 nM for M2 and 189 nM for M6, thus, virtually identical to that of the wt protein. Altogether, these data showed that the TG2 heparin binding site is a composite one, as both clusters 262–265 (M1) on one side and 598–602 (M3) on the other side are strictly required for the interaction to take place, with a participation of residues 19 (M4), 28 (M5), and 634 (M7).

Binding of Conformationally Open and Closed TG2 to Heparin—In the folded conformation the two positive clusters 262–265 (M1) and 598–602 (M3) are spatially close (Fig. 1), whereas in the open "active" conformation these sites are spatially distant (41). To investigate the affinity of TG2 for heparin

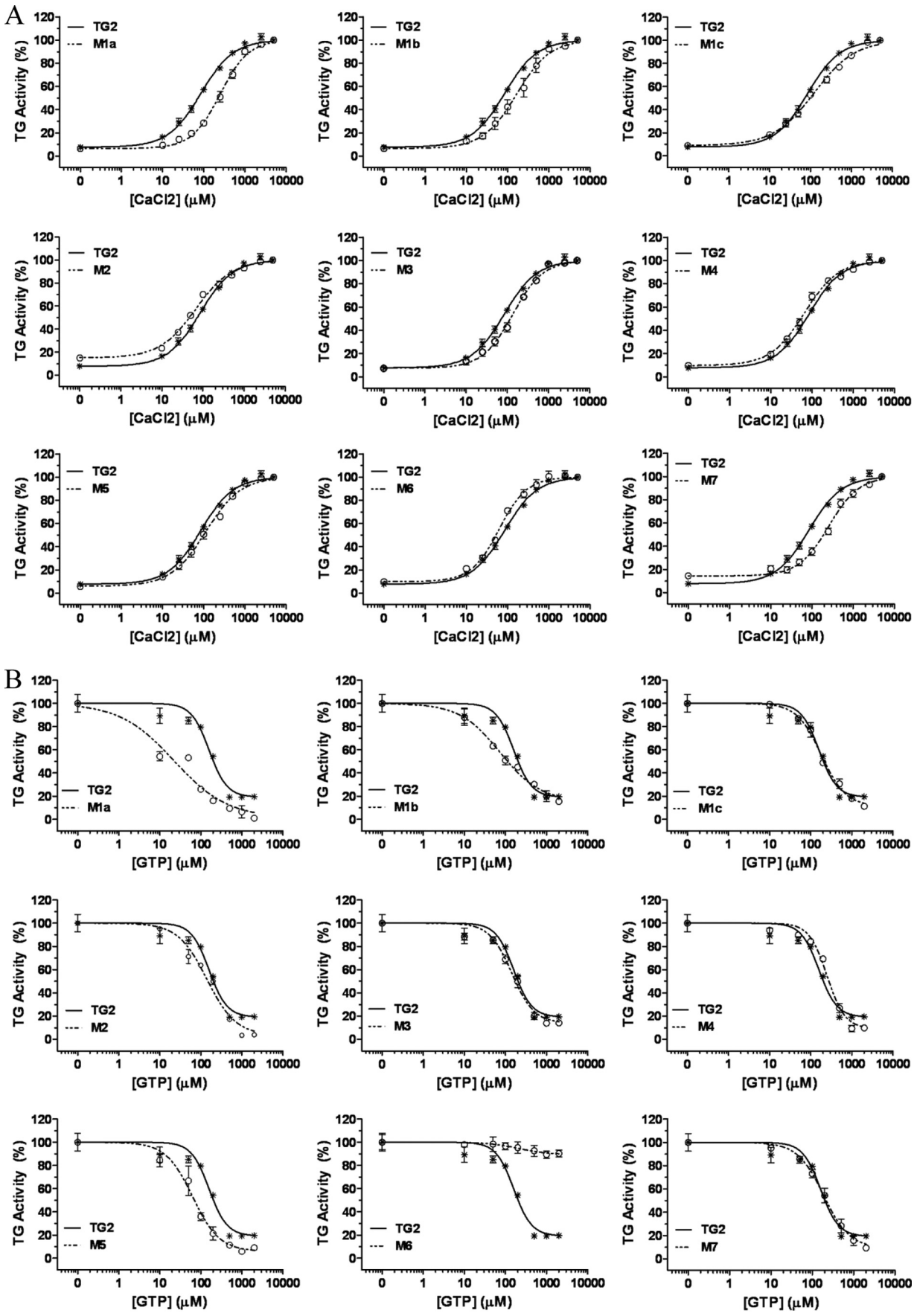
A
TG2
M1a
M1b
M1c
M2
M3
M4
M5
M6
M7
TG Activity (%)
[CaCl2] (μM)
B
[GTP] (μM)

in the open and closed conformation, we stabilized TG2 in the open form by alkylation of the active site using two different TG2 inhibitors, R283 and Boc-DON, as described under "Experimental Procedures." TG2 in complex with either the covalently bound inhibitors displayed strongly reduced binding to heparin compared with untreated TG2 (Fig. 4*A*). This finding was further investigated by comparing the heparin binding properties of the Open-tTG^{TM}, a commercially available His-tagged TG2 whose open conformation is experimentally confirmed, with that of His-tagged wt TG2 produced by the same manufacturer (Fig. 4*B*). Our data show that TG2 does not bind heparin in the linear open structure.

Docking Calculations—The low energy conformers of the pentasaccharide mimicking heparin were docked in the TG2 model as described under "Experimental Procedures." The resulting poses were ranked according to their Glide scores that ranged between −5.2 and −2. Five representative solutions from the docking calculations are displayed in Fig. 5*A*. All five pentasaccharides lie in a crevasse at the protein surface that is surrounded by basic amino acids. Each pentasaccharide does not interact with all of the basic amino acids that are labeled in Fig. 5*A*, but with a subset of them, depending upon their localization and orientation. Among the five pentasaccharides, the (φ, ψ) angles of the iduronic acid-GlcN bond and of the iduronic acid-GlcN bond are centered around values of (−71° ± 11, 111° ± 60) and (67° ± 22, 63° ± 37), respectively. The average values are similar to the ones observed in many heparin-bound crystal complexes (42), and the deviations are mostly on the ψ angle, in agreement with the previously calculated energy maps of the heparin disaccharides (43). The bound conformations present, therefore, some flexibility ranging from a fully extended shape to a curved shape.

The solution displayed in Fig. 5*B* has been selected among the Glide high scores on the basis of its strong interaction with basic amino acids and its extended shape. The position of reducing and non-reducing end could be easily extended to a polysaccharide. The selected solution demonstrates that a pentasaccharide can easily establish strong salt bridges between sulfate or acidic groups and the basic amino acids Arg^{28}, Arg^{262}, Arg^{263}, Lys^{265}, Lys ^{600}, and Lys^{634}. Additional hydrogen bonds are rare. In this pose they appear only between *N*-sulfate and Asn^{266} and between O-2 of iduronic acid and Gln^{633} (not shown). Arg^{262} has a central location in the basic patch constituted by Arg^{262}, Arg^{263}, Lys^{265} and establishes contacts not only with the sulfate group of central iduronic residue but also with the ring oxygen.

Analyses of the 16 best docking poses (Fig. 5, *A* and *C*) demonstrated the plasticity of the interaction. The basic amino acids described above are generally involved in contact with a sulfate but not to a specific one in the pentasaccharide sequence.

Importance of TG2-Heparin Binding Site in Support of TG2-mediated RGD-independent Cell Adhesion—We have previously shown that extracellular matrix TG2 supports RGD-independent cell adhesion and that this represents a rescue cell pathway in situations of matrix fragmentation during tissue repair, when TG2 is abundantly deposited in a protease-resistant complex with fibronectin (19, 20). Cell binding to TG2-fibronectin requires a direct interaction of TG2 with the HS chains of sdc-4 (23). It is, therefore, anticipated that ligation of cell surface sdc-4 by the heparin binding site of TG2 would be required. Having identified the heparin-binding site within TG2, we investigated the effects of its mutation in TG2-mediated RGD-independent cell adhesion. For these studies we used Swiss 3T3 fibroblasts as a cell model (19). Among the heparin binding mutant TG2 proteins, we tested M1c, corresponding to the first BBXB cluster (Lys^{265}), and M3, corresponding to the second heparin binding cluster BXBBB (Lys^{598}/Lys^{600}/Arg^{601}/Lys^{602}). As showed earlier in this study, these mutants had no residual heparin binding affinity (Fig. 3) and were biochemically very similar to the wt enzyme (Fig. 2). We also included TG2 mutants with retained heparin binding properties, M2, corresponding to Lys^{202}/Lys^{205}, and M6, corresponding to Arg^{580}. wt and mutant TG2 proteins were allowed to associate with fibronectin as previously described (19, 20). Measurements of TG2 bound to fibronectin by an ELISA-type assay showed similar fibronectin associations between wt and mutant TG2 proteins (supplemental Fig. 3*A*). Next, cells were allowed to adhere on fibronectin alone or fibronectin supplemented with either wt or mutant TG2 proteins, in the presence of competitive concentrations of soluble RGD peptide or control inactive RAD peptide (19, 20). As shown in Fig. 6, by blocking fibronectin binding to $\alpha_5\beta_1$ integrins, the RGD peptide significantly reduced cell attachment and spreading on fibronectin (FN) to ~50% that of the control value (FN with or without RAD peptide). In contrast, the RGD peptide did not significantly compete with $\alpha_5\beta_1$ integrin-cell attachment and spreading when cells were seeded on fibronectin in complex with wt TG2 (FN-TG2), which was conducive of RGD-independent cell adhesion, as previously shown (19). However, when cells were allowed to adhere on fibronectin in complex with the heparin binding TG2 mutants (FN-M1c and FN-M3) in the presence of RGD peptide, cells only reached ~half the control cell attachment and spreading values (FN with or without RAD peptide). The TG2 mutants with retained heparin binding (FN-M2 and FN-M6) still supported RGD-independent cell adhesion. In conclusion, the heparin binding TG2 mutants M1c and M3 failed to compensate the loss of RGD dependence in terms of number of attached cells and cytosolic morphology. The result shows that the heparin binding site of TG2 that we have identified is responsible for stimulating RGD-independent cell adhesion.

FIGURE 2. **Calcium activation and GTP inhibition of wt and mutant TG2 activity.** *A*, the transamidating activity of TG2 (13 nM) was assayed at increasing Ca^{2+} concentrations (10, 25, 50, 100, 250, 500, 1000, 2500, 5000 μM) as described under "Experimental Procedures." *B*, TG transamidation was assayed at increasing concentrations of GTP (10, 50, 100, 200, 500, 1000, 2000 μM) in the presence of 150 μM Ca^{2+}. Data are expressed as a percentage of the maximal TG activity for each protein and are presented as the mean ± S.E. of five (*A*) and three (*B*) independent experiments carried out in triplicate. Sigmoid curves were fitted to "sigmoid dose-response (variable slope)" using GraphPad Prism. R^2 was ≥ 0.93.

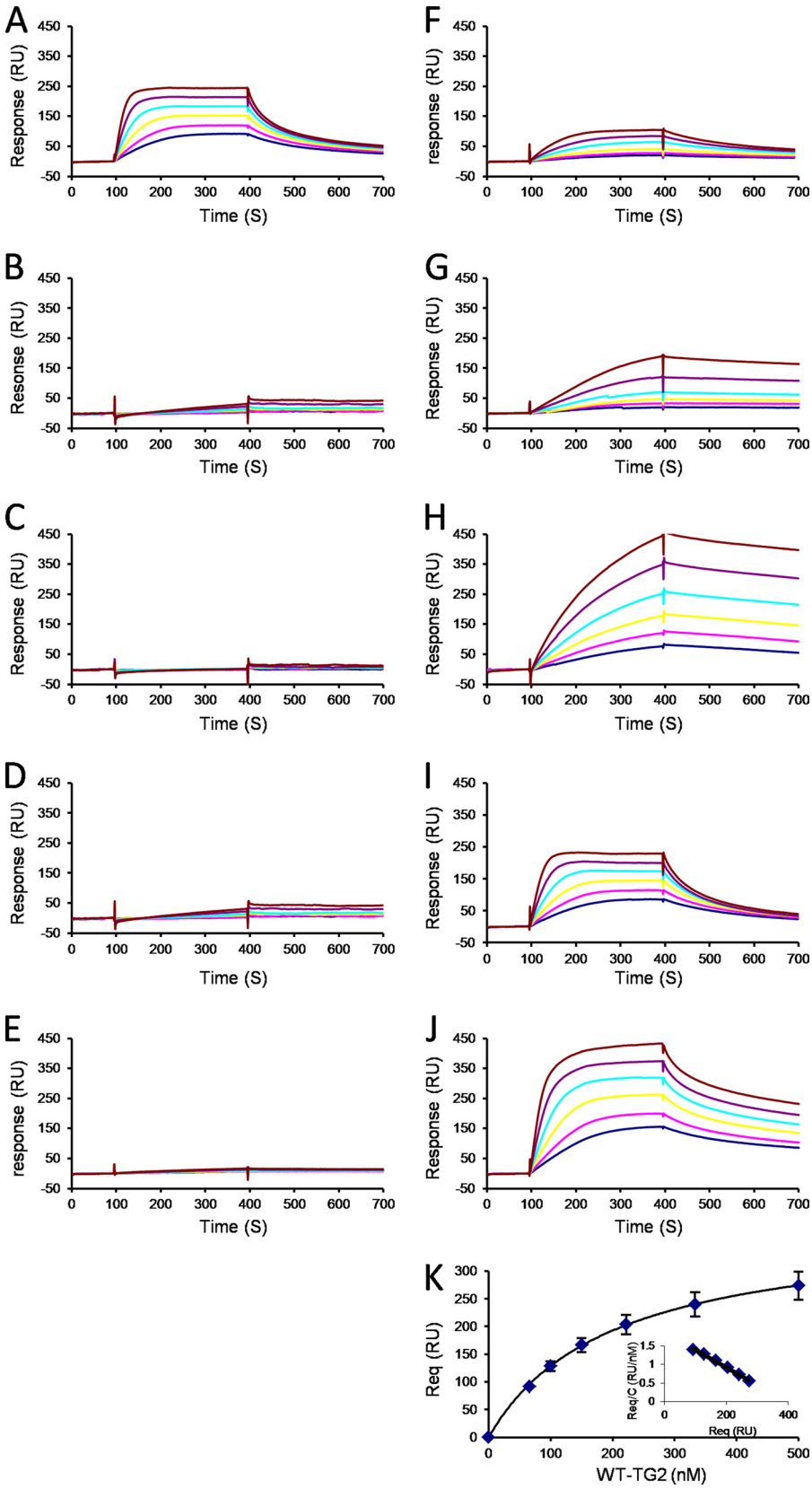

FIGURE 3. **Binding of wt and mutant TG2 to immobilized heparin.** Wt TG2 (*A*), mutants M1a (*B*), M1b (*C*), M1c (*D*), M3 (*E*), M4 (*F*), M5 (*G*), M7 (*H*), M2 (*I*), and M6 (*J*) were injected over a heparin-activated surface at a flow rate or 20 μl/min for 5 min, after which running buffer was injected, and the response in resonance units was recorded as a function of time. Each set of sensorgrams was obtained with TG2 molecules at (from *top* to *bottom*) 500, 333, 222, 150, 100, and 66 nM. *K*, steady state values at equilibrium plotted against the injected concentration of WT-TG2 and fitted to $R_{eq} = R\max_{eq}/(K_D + c)$ are shown. *Inset*, Scatchard plot (R_{eq}/c *versus* R_{eq}) of the corresponding data. R_{eq} values are the steady state values at equilibrium recorded at the end of the association phase, and *c* is the concentration of injected proteins. Samples for which the association phase reached equilibrium (wt, M2, and M6) were analyzed similarly. Experiments were performed in duplicate.

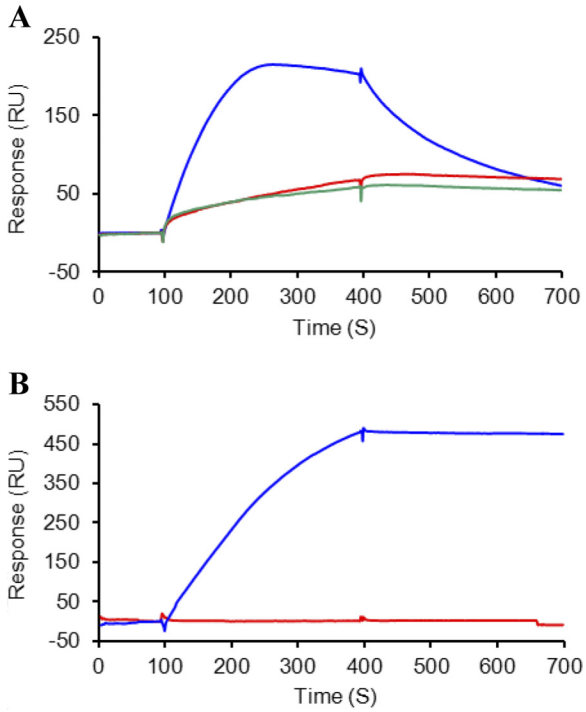

FIGURE 4. **Binding of open TG2 to immobilized heparin.** *A*, wt TG2 either stabilized in the open conformation by the inhibitors R283 (*red trace*) and Boc-DON (*green trace*) in the presence of 10 mM Ca^{2+} or assayed in buffer with 2 mM EDTA (*blue trace*) is shown. *B*, Open-tTG^{TM} (*red trace*) and commercial wt TG2 in buffer with 2 mM EDTA (*blue trace*) is shown. Proteins were injected at 200 nM over a heparin-activated surface and analyzed as described in Fig. 3.

Although the structure of fibronectin-bound TG2 is not known, by measuring its transamidating activity in cell culture medium we have confirmed that, when immobilized on fibronectin, His-tagged TG2 loses most of its transamidating activity despite activating concentrations of Ca^{2+} in DMEM (1.8 mM). The activity is only partly regained by the addition of DTT (supplemental Fig. 3*B*) (19). In this form fibronectin-associated TG2 retains heparin recognition compared with fibronectin-associated Open-tTG^{TM} when assayed at equilibrium by plate binding assay (supplemental Fig. 3*C*) (23). We conclude that within the fibronectin-TG2 heterocomplex, TG2 bears an inactive conformation with retained heparin binding.

DISCUSSION

There is evidence that HS proteoglycans mediate the biological activity of TG2 in at least two ways; first, by controlling TG2 cell surface trafficking and externalization (23), and second, by acting as cell surface adhesion receptors for TG2 once it is released and deposited in a heterocomplex with FN (19, 20, 25). As an increased externalization of TG2 has been implicated in several different pathologies, investigating the nature of the TG2-HS association is important to assist in determining its physiological role *in vivo* and to allow the rational control of this interaction. We have previously reported that TG2 interacts with HS or its highly sulfated analog heparin strongly, with low nanomolar K_D values (23). Here we have investigated the nature of the binding site and characterized, for the first time, the residues involved in this interaction.

Analysis of the three-dimensional structure of TG2 protein revealed clusters of positively charged amino acids on the TG2 surface forming typical heparin binding sequences (38) and spatially close individual basic amino acids that are potentially accessible by HS chains. Testing these positions of possible HS binding by site-directed mutagenesis revealed that mutation of basic cluster KQKRK (598–602) was associated with an almost complete reduction of heparin binding (Biacore analysis) compared with the wt enzyme. It also showed that mutation of the

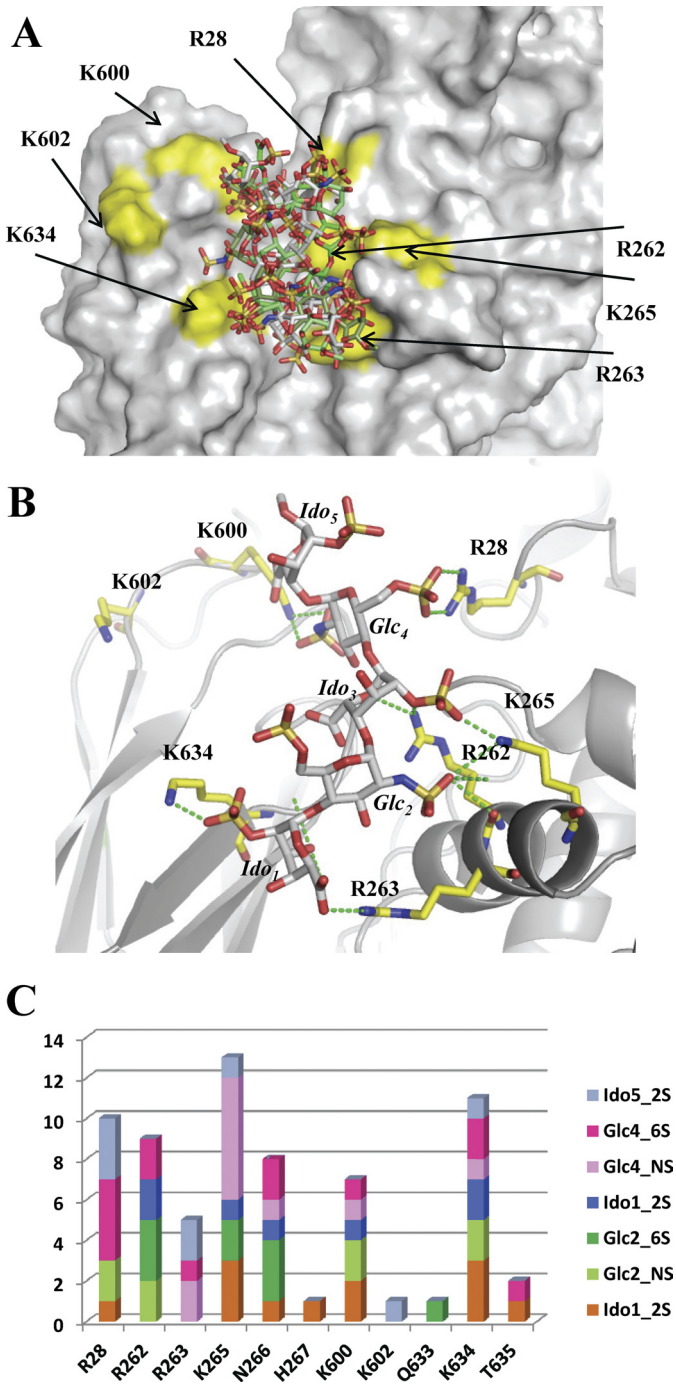

FIGURE 5. *A*, shown is superposition of the accessible surface of TG2 with five docked pentasaccharides selected among the 16 with higher GLIDE scores and representing the range of available conformations. *B*, selection of one pose among the 16 best ones with representation of hydrogen bonds to basic amino acids is shown. *C*, shown is the total number of hydrogen bonds for the 16 best poses as a function of the involved carbohydrate sulfate group and protein amino acid.

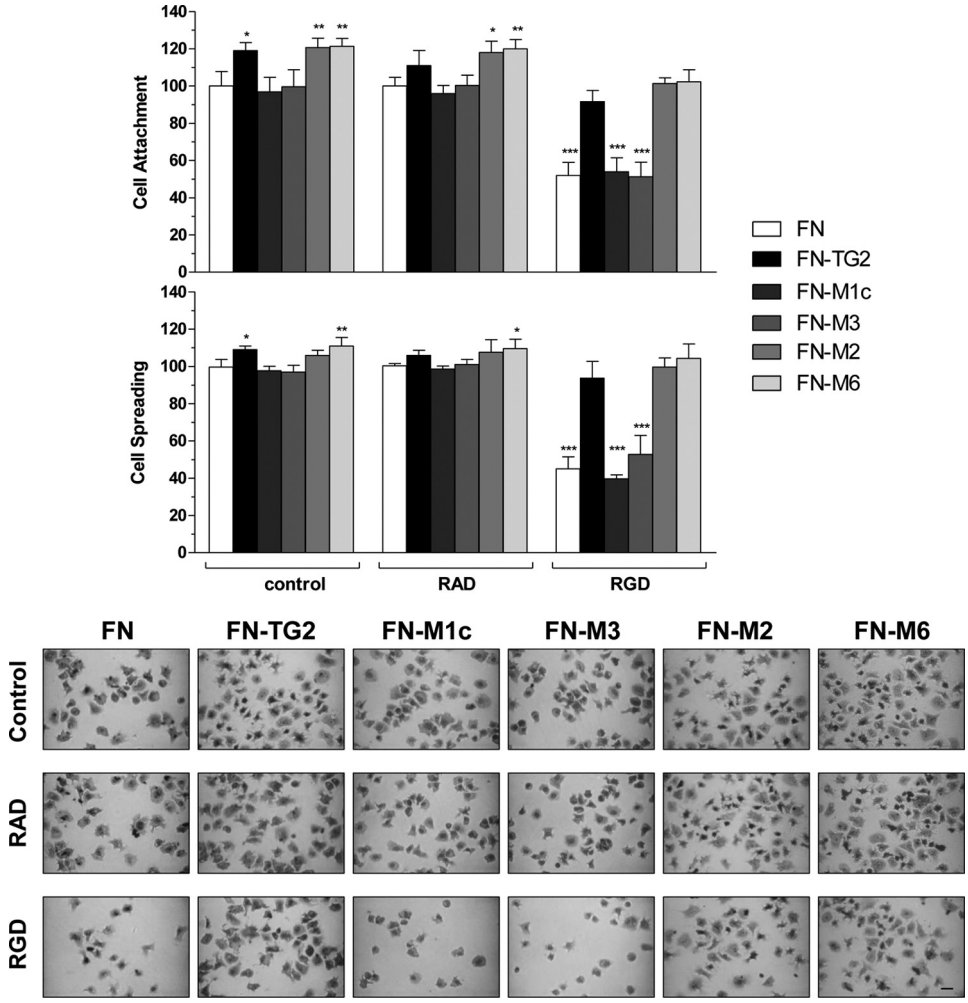

FIGURE 6. **RGD-independent cell adhesion of wt TG2 and TG2 heparin binding mutants.** Swiss 3T3 fibroblasts were allowed to adhere either on FN alone or FN supplemented with wt or mutant TG2 (heparin binding mutants M1c and M3; mutants with retained heparin-binding M2 and M6) in serum-free medium for 20 min as described under "Experimental Procedures." Where indicated cells were preincubated with competitive concentrations of soluble GRGDTP peptide or control GRADSP peptide (100 μg/ml). The degree of cell adhesion was assessed on fixed cells stained with May Grunwald/Giemsa, shown in the *bottom panel*, as previously described (19). Each point represents the mean number of attached cells (cell attachment) or mean percentage of spread cells (cell spreading) $\pm$ S.D. of a representative experiment undertaken in triplicate. Data are expressed as the percentage of control values on FN, which represents 100%. Before normalization, mean attachment values $\pm$ S.D. on FN control were 415 $\pm$ 33. Mean percentage values of spread cells on FN were 81 $\pm$ 3; the total number of quantified cells in the control ranged from 400 to 500 cells in all the type of matrices. Bar, 20 μm.

individual basic residues Arg^{262}, Arg^{263}, and Lys^{265}, forming a second positively charged RRWK cluster (262–265), was sufficient to lead to a large reduction in heparin binding. Mutation of basic residues Arg^{19} and Arg^{28}, which in the crystal structure are located next to the two above-mentioned clusters, also led to a significant reduction in heparin binding, suggesting their involvement. Mutation of Lys^{634}, which is also spatially closed to these two clusters, led to a slower rate of binding to heparin, showing the involvement of this further residue in heparin interaction. In contrast, neither Lys^{202} and Lys^{205} residues nor the GTP binding site Arg^{580}, which constitutes further accessible basic sites, was shown to participate in heparin binding.

Our study has led us to conclude that the heparin binding site on TG2 mainly comprises two clusters of basic amino acids, the RRWK (262–265) and the KQKRK (598–602). These two positive clusters are distant in the linear sequence; however, they are brought into spatial proximity on the folded closed protein, forming the heparin binding site. In this conformation TG2 is typically bound to guanine or adenine nucleotide and its active site (Cys^{277}-His^{335}-Asp^{358} catalytic triad) is obscured as a result of guanine nucleotide or adenine nucleotide binding (28, 29).

In its active conformation, which was resolved on TG2 bound to irreversible active-site inhibitors, Ca^{2+} binding involves a large conformational change (41). Although in the folded conformation the two positive sequences, RRWK (262–265) and KQKRK (598–602), are spatially close, in the open active conformation they are spatially distant. Based on the finding that mutations in these individual clusters very strongly impaired heparin binding and, thus, that they both contribute to form a single binding surface, it could be concluded that the open form has a reduced heparin binding affinity compared with the closed conformation. We tested this hypothesis and found that the open TG2 form displayed a strongly reduced ability to bind to heparin compared with the closed one. This finding supports the view that TG2 features two independent heparin binding sites, which are brought into close proximity in the closed protein, forming a large interacting basic surface, which is destroyed by the

opening of the structure. This result is also consistent with the fact that mutations in a single domain are sufficient to knock down heparin binding. However, such a drastic effect of a single point mutation on heparin binding has been observed already, for example, in the chemokine stromal cell-derived factor-1, where two single mutations were each able to almost fully inhibit HS recognition (44).

We have also shown that a single heparin-derived pentasaccharide has the length required to make contacts with the residues of the two basic clusters, RRWK (262–265) and KQKRK (598–602), of TG2 in the closed conformation. *In vivo* HS are present as syndecan or glypican receptors at the cell surface and perlecans in the basement membranes (27). Further studies will be necessary to identify the HS sequences interacting with TG2 and whether the nature of the HS chains composition and their tissue concentration affects the trafficking/biological activity of TG2 in different cell compartments.

TG2 is mostly regarded as a latent enzyme whose activity is kept under tight control to prevent excessive post-translational modifications of protein substrates (12, 45). A demonstration of this is given by the comparable level of Ca^{2+}-dependent TG2 transamidation obtained from conditioned matrices with low levels of TG2 and matrices with high levels of TG2, suggesting that TG activity is transient and it is down-regulated by matrix sequestration (19). There is a clear mechanism of TG2 regulation inside the cells, as Ca^{2+}-dependent transamidation is allosterically inhibited by guanine nucleotide binding and a low Ca^{2+}-nucleotide ratio. However, outside the cell where TG2 is potentially constantly activated by high (millimolar) concentrations of Ca^{2+} resulting into a high Ca^{2+}-nucleotide ratio, the mechanism of TG2 regulation it is less clear. Oxidation of TG2 and formation of critical disulfide bonds may contribute to its extracellular regulation causing loss of TG2 activity (46), which can be restored by reducing agents (47). It has also been suggested that nitrosylation of TG2 via NO may contribute to its transition between active enzyme and "structural matrix protein" with no required transamidating activity (48). It could be speculated that short *N*-sulfoglucosamine-enriched HS sequences, bridging the RRWK (262–265) and KQKRK (598–602) sites, could stabilize the closed form and that high calcium concentrations might indeed partially disrupt the complex and thus favor the transition toward the open active form. In this way the interaction with HS may regulate TG2 activity depending on Ca^{2+}/HS microenvironment. An example of regulation of enzymatic activity by HS and ionic changes was previously reported for elastase and cathepsin G, which are stored in an inactive form, bound to HS proteoglycans within neutrophil granules, and released in an active form by an increase of ionic strength (K^+ ions) (49). Thus, regulation of TG2 activity in the extracellular environment may be linked to structural changes brought about by HS proteoglycans structures and Ca^{2+} ions. We previously suggested that HSs regulate the cell surface trafficking of TG2 as the absence of cell surface HS or cells with targeted deletion of sdc-4 do not effectively externalize TG2 (23, 25). As described for FGF (50), HS may be effective in trapping and anchoring leaderless TG2 once exported to the cell surface. In this scenario, the activating concentration of Ca^{2+} in the extracellular space could destabilize the closed form and the HS interaction, leading to the "release" of active TG2. Therefore, binding of TG2 to HS via the identified binding site may be another level of control for extracellular TG2 and have widespread biological consequences/implications, particularly in the context of cell adhesion, tissue fibrosis, and cancer progression.

We know that matrix TG2 when in heterocomplex with fibronectin supports RGD-independent cell adhesion through ligation of the HS chains of sdc-4. In this study we have shown that mutant forms of TG2 lacking either of the two identified heparin binding clusters supported only weak RGD-independent cell adhesion compared with wt TG2 or TG2 mutants with retained heparin binding properties. This finding suggests the requirement for both heparin binding clusters, RRWK (262–265) and KQKRK (598–602), for TG2-mediated cell adhesion. It also substantiates evidence that the cell surface receptor for matrix TG2 is a heparan sulfate proteoglycan, corroborating the knowledge that HS chains regulate the biological function of TG2 at many levels. Although we do not know which conformation TG2 assumes in heterocomplex with fibronectin, we have confirmed that TG2 becomes a catalytically inactive "structural" protein, which we conclude retains heparin binding.

Multiple alignments of the human, mouse, and rat TG2 protein have revealed that the two positive clusters forming the heparin binding site in the human TG2 sequence are mostly conserved, with the exception of Lys^{600}, within the KQKRK (598–602) motif, which is a neutral amino acid (Asn) in rat and mouse TG2. Among the other contributing residues, Arg^{19} is conserved among the different species, but residue Arg^{28} is a neutral Gln in rat and mouse TG2. Sequence alignments of human TG1, TG2, TG3, TG4, TG5, TG6, TG7, and FXIIIa revealed no obvious homology of the heparin binding sites with consensus *X*BB*X*B*X* and *X*BBB*XX*B*X* (38) identified in TG2, with the exception of KQKRK (598–602) in TG3, which is replaced by another positive cluster (RVRK), and the basic residue Arg-19, which is conserved in TG1. Our preliminary observations (Biacore analysis) indicate that among the TG family members we have analyzed, only TG2 and TG1 bind heparin with high affinity (TG3 and FXIIIa have low heparin binding affinity). Because the full site is not conserved in TG1, we conclude that TG2 has a unique heparin binding site within the family of transglutaminases that could be specifically targeted to control the TG2-HS interaction.

In summary, we have mapped high affinity heparin binding sites on TG2 that are brought into close proximity on the folded protein and demonstrated that they influence RGD-independent cell adhesion mediated by TG2-fibronectin heterocomplex. These data have provided novel insights into the molecular nature of HS/heparin interaction with TG2 creating new a hypothesis on how heparan sulfate proteoglycans could regulate the extracellular function of TG2.

Acknowledgments—We thank the Partnership for Structural Biology-platforms for Biacore time and Cyril Bras (Centre de Recherches sur les Macromolécules Végétales-CNRS) for helpful technical support. We are grateful to Dr. Marjolaine Noirclerc-Savoye from the Institut de Biologie Structurale-platform of the Partnership for Structural Biology for access to Thermal Shift Assay facilities.

REFERENCES

1. Iismaa, S. E., Mearns, B. M., Lorand, L., and Graham, R. M. (2009) Transglutaminases and disease. Lessons from genetically engineered mouse models and inherited disorders. *Physiol. Rev.* **89,** 991–1023
2. Radisky, D. C., Stallings-Mann, M., Hirai, Y., and Bissell, M. J. (2009) Single proteins might have dual but related functions in intracellular and extracellular microenvironments. *Nat. Rev. Mol. Cell Biol.* **10,** 228–234
3. Belkin, A. M. (2011) Extracellular TG2. Emerging functions and regulation. *FEBS J.* **278,** 4704–4716
4. Verderio, E. A., Johnson, T., and Griffin, M. (2004) Tissue transglutaminase in normal and abnormal wound healing. Review article. *Amino Acids* **26,** 387–404
5. Jang, G. Y., Jeon, J. H., Cho, S. Y., Shin, D. M., Kim, C. W., Jeong, E. M., Bae, H. C., Kim, T. W., Lee, S. H., Choi, Y., Lee, D. S., Park, S. C., and Kim, I. G. (2010) Transglutaminase 2 suppresses apoptosis by modulating caspase 3 and NF-κB activity in hypoxic tumor cells. *Oncogene* **29,** 356–367
6. Shin, D. M., Jeon, J. H., Kim, C. W., Cho, S. Y., Lee, H. J., Jang, G. Y., Jeong, E. M., Lee, D. S., Kang, J. H., Melino, G., Park, S. C., and Kim, I. G. (2008) TGFβ mediates activation of transglutaminase 2 in response to oxidative stress that leads to protein aggregation. *FASEB J.* **22,** 2498–2507
7. Satpathy, M., Shao, M., Emerson, R., Donner, D. B., and Matei, D. (2009) Tissue transglutaminase regulates matrix metalloproteinase-2 in ovarian cancer by modulating cAMP-response element-binding protein activity. *J. Biol. Chem.* **284,** 15390–15399
8. Antonyak, M. A., Li, B., Regan, A. D., Feng, Q., Dusaban, S. S., and Cerione, R. A. (2009) Tissue transglutaminase is an essential participant in the epidermal growth factor-stimulated signaling pathway leading to cancer cell migration and invasion. *J. Biol. Chem.* **284,** 17914–17925
9. Hwang, J. Y., Mangala, L. S., Fok, J. Y., Lin, Y. G., Merritt, W. M., Spannuth, W. A., Nick, A. M., Fiterman, D. J., Vivas-Mejia, P. E., Deavers, M. T., Coleman, R. L., Lopez-Berestein, G., Mehta, K., and Sood, A. K. (2008) Clinical and biological significance of tissue transglutaminase in ovarian carcinoma. *Cancer Res.* **68,** 5849–5858
10. Johnson, T. S., El-Koraie, A. F., Skill, N. J., Baddour, N. M., El Nahas, A. M., Njloma, M., Adam, A. G., and Griffin, M. (2003) Tissue transglutaminase and the progression of human renal scarring. *J. Am. Soc. Nephrol.* **14,** 2052–2062
11. Jeitner, T. M., Pinto, J. T., Krasnikov, B. F., Horswill, M., and Cooper, A. J. (2009) Transglutaminases and neurodegeneration. *J. Neurochem.* **109,** 160–166
12. Lorand, L., and Graham, R. M. (2003) Transglutaminases. Cross-linking enzymes with pleiotropic functions. *Nat. Rev. Mol. Cell Biol.* **4,** 140–156
13. Hadjivassiliou, M., Sanders, D. S., Grünewald, R. A., Woodroofe, N., Boscolo, S., and Aeschlimann, D. (2010) Gluten sensitivity. From gut to brain. *Lancet Neurol.* **9,** 318–330
14. Begg, G. E., Carrington, L., Stokes, P. H., Matthews, J. M., Wouters, M. A., Husain, A., Lorand, L., Iismaa, S. E., and Graham, R. M. (2006) Mechanism of allosteric regulation of transglutaminase 2 by GTP. *Proc. Natl. Acad. Sci. U.S.A.* **103,** 19683–19688
15. Nakaoka, H., Perez, D. M., Baek, K. J., Das, T., Husain, A., Misono, K., Im, M. J., and Graham, R. M. (1994) Gh, a GTP-binding protein with transglutaminase activity and receptor signaling function. *Science* **264,** 1593–1596
16. Verderio, E., Nicholas, B., Gross, S., and Griffin, M. (1998) Regulated expression of tissue transglutaminase in Swiss 3T3 fibroblasts. Effects on the processing of fibronectin, cell attachment, and cell death. *Exp. Cell Res.* **239,** 119–138
17. Balklava, Z., Verderio, E., Collighan, R., Gross, S., Adams, J., and Griffin, M. (2002) Analysis of tissue transglutaminase function in the migration of Swiss 3T3 fibroblasts. The active-state conformation of the enzyme does not affect cell motility but is important for its secretion. *J. Biol. Chem.* **277,** 16567–16575
18. Akimov, S. S., Krylov, D., Fleischman, L. F., and Belkin, A. M. (2000) Tissue transglutaminase is an integrin binding adhesion coreceptor for fibronectin. *J. Cell Biol.* **148,** 825–838
19. Verderio, E. A., Telci, D., Okoye, A., Melino, G., and Griffin, M. (2003) A novel RGD-independent cel adhesion pathway mediated by fibronectin-bound tissue transglutaminase rescues cells from anoikis. *J. Biol. Chem.* **278,** 42604–42614
20. Telci, D., Wang, Z., Li, X., Verderio, E. A., Humphries, M. J., Baccarini, M., Basaga, H., and Griffin, M. (2008) Fibronectin tissue transglutaminase matrix rescues RGD-impaired cell adhesion through syndecan-4 and β1 integrin co-signaling. *J. Biol. Chem.* **283,** 20937–20947
21. Király, R., Demény, M., and Fésüs, L. (2011) Protein transamidation by transglutaminase 2 in cells. A disputed Ca^{2+}-dependent action of a multifunctional protein. *FEBS J.* **278,** 4717–4739
22. Zemskov, E. A., Mikhailenko, I., Hsia, R. C., Zaritskaya, L., and Belkin, A. M. (2011) Unconventional secretion of tissue transglutaminase involves phospholipid-dependent delivery into recycling endosomes. *PLoS One* **6,** e19414
23. Scarpellini, A., Germack, R., Lortat-Jacob, H., Muramatsu, T., Billett, E., Johnson, T., and Verderio, E. A. (2009) Heparan sulfate proteoglycans are receptors for the cell-surface trafficking and biological activity of transglutaminase-2. *J. Biol. Chem.* **284,** 18411–18423
24. Verderio, E. A., Scarpellini, A., and Johnson, T. S. (2009) Novel interactions of TG2 with heparan sulfate proteoglycans. reflection on physiological implications. *Amino Acids* **36,** 671–677
25. Verderio, E., and Scarpellini, A. (2010) Significance of the syndecan-4-transglutaminase-2 interaction. *ScientificWorldJournal* **10,** 1073–1077
26. Yu, Y., Sweeney, M. D., Saad, O. M., Crown, S. E., Hsu, A. R., Handel, T. M., and Leary, J. A. (2005) Chemokine-glycosaminoglycan binding. Specificity for CCR2 ligand binding to highly sulfated oligosaccharides using FTICR mass spectrometry. *J. Biol. Chem.* **280,** 32200–32208
27. Bishop, J. R., Schuksz, M., and Esko, J. D. (2007) Heparan sulfate proteoglycans fine-tune mammalian physiology. *Nature* **446,** 1030–1037
28. Liu, S., Cerione, R. A., and Clardy, J. (2002) Structural basis for the guanine nucleotide-binding activity of tissue transglutaminase and its regulation of transamidation activity. *Proc. Natl. Acad. Sci. U.S.A.* **99,** 2743–2747
29. Han, B. G., Cho, J. W., Cho, Y. D., Jeong, K. C., Kim, S. Y., and Lee, B. I. (2010) Crystal structure of human transglutaminase 2 in complex with adenosine triphosphate. *Int. J. Biol. Macromol.* **47,** 190–195
30. Gentile, V., Saydak, M., Chiocca, E. A., Akande, O., Birckbichler, P. J., Lee, K. N., Stein, J. P., and Davies, P. J. (1991) Isolation and characterization of cDNA clones to mouse macrophage and human endothelial cell tissue transglutaminases. *J. Biol. Chem.* **266,** 478–483
31. Piper, J. L., Gray, G. M., and Khosla, C. (2002) High selectivity of human tissue transglutaminase for immunoactive gliadin peptides. Implications for celiac sprue. *Biochemistry* **41,** 386–393
32. Rossi, V., Bally, I., Ancelet, S., Xu, Y., Frémeaux-Bacchi, V., Vivès, R. R., Sadir, R., Thielens, N., and Arlaud, G. J. (2010) Functional characterization of the recombinant human C1 inhibitor serpin domain. Insights into heparin binding. *J. Immunol.* **184,** 4982–4989
33. Niesen, F. H., Berglund, H., and Vedadi, M. (2007) The use of differential scanning fluorimetry to detect ligand interactions that promote protein stability. *Nat. Protoc.* **2,** 2212–2221
34. Jones, R. A., Nicholas, B., Mian, S., Davies, P. J., and Griffin, M. (1997) Reduced expression of tissue transglutaminase in a human endothelial cell line leads to changes in cell spreading, cell adhesion, and reduced polymerisation of fibronectin. *J. Cell Sci.* **110,** 2461–2472
35. Kaminski, G. A., Friesner, R. A., Tirado-Rives, J., and Jorgensen, W. L. (2001) Evaluation and reparametrization of the OPLSAA force field for proteins via comparison with accurate quantum chemical calculations on peptides. *J. Phys. Chem. B* **105,** 6474–6487
36. Mulloy, B., Forster, M. J., Jones, C., and Davies, D. B. (1993) NMR and molecular-modeling studies of the solution conformation of heparin. *Biochem. J.* **293,** 849–858
37. Friesner, R. A., Banks, J. L., Murphy, R. B., Halgren, T. A., Klicic, J. J., Mainz, D. T., Repasky, M. P., Knoll, E. H., Shelley, M., Perry, J. K., Shaw, D. E., Francis, P., and Shenkin, P. S. (2004) Glide: a new approach for rapid, accurate docking and scoring. 1. Method and assessment of docking accuracy. *J. Med. Chem.* **47,** 1739–1749
38. Cardin, A. D., Jackson, R. L., Sparrow, D. A., and Sparrow, J. T. (1989) Interaction of glycosaminoglycans with lipoproteins. *Ann. N.Y. Acad. Sci.* **556,** 186–193
39. Vivès, R. R., Crublet, E., Andrieu, J. P., Gagnon, J., Rousselle, P., and Lortat-

Jacob, H. (2004) A novel strategy for defining critical amino acid residues involved in protein/glycosaminoglycan interactions. *J. Biol. Chem.* **279,** 54327–54333
40. Begg, G. E., Holman, S. R., Stokes, P. H., Matthews, J. M., Graham, R. M., and Iismaa, S. E. (2006) Mutation of a critical arginine in the GTP-binding site of transglutaminase 2 disinhibits intracellular cross-linking activity. *J. Biol. Chem.* **281,** 12603–12609
41. Pinkas, D. M., Strop, P., Brunger, A. T., and Khosla, C. (2007) Transglutaminase 2 undergoes a large conformational change upon activation. *PLoS Biol.* **5,** e327
42. Khan, S., Gor, J., Mulloy, B., and Perkins, S. J. (2010) Semi-rigid solution structures of heparin by constrained X-ray scattering modeling. New insight into heparin-protein complexes. *J. Mol. Biol.* **395,** 504–521
43. Cros, S., Petitou, M., Sizun, P., Pérez, S., and Imberty, A. (1997) Combined NMR and molecular modeling study of an iduronic acid-containing trisaccharide related to antithrombotic heparin fragments. *Bioorg. Med. Chem.* **5,** 1301–1309
44. Sadir, R., Baleux, F., Grosdidier, A., Imberty, A., and Lortat-Jacob, H. (2001) Characterization of the stromal cell-derived factor-1α-heparin complex. *J. Biol. Chem.* **276,** 8288–8296
45. Siegel, M., Strnad, P., Watts, R. E., Choi, K., Jabri, B., Omary, M. B., and Khosla, C. (2008) Extracellular transglutaminase 2 is catalytically inactive but is transiently activated upon tissue injury. *PLoS One* **3,** e1861
46. Stamnaes, J., Pinkas, D. M., Fleckenstein, B., Khosla, C., and Sollid, L. M. (2010) Redox regulation of transglutaminase 2 activity. *J. Biol. Chem.* **285,** 25402–25409
47. Jin, X., Stamnaes, J., Klöck, C., DiRaimondo, T. R., Sollid, L. M., and Khosla, C. (2011) Activation of extracellular transglutaminase 2 by thioredoxin. *J. Biol. Chem.* **286,** 37866–37873
48. Telci, D., Collighan, R. J., Basaga, H., and Griffin, M. (2009) Increased TG2 expression can result in induction of transforming growth factor β1, causing increased synthesis and deposition of matrix proteins, which can be regulated by nitric oxide. *J. Biol. Chem.* **284,** 29547–29558
49. Reeves, E. P., Lu, H., Jacobs, H. L., Messina, C. G., Bolsover, S., Gabella, G., Potma, E. O., Warley, A., Roes, J., and Segal, A. W. (2002) Killing activity of neutrophils is mediated through activation of proteases by K^+ flux. *Nature* **416,** 291–297
50. Zehe, C., Engling, A., Wegehingel, S., Schäfer, T., and Nickel, W. (2006) Cell-surface heparan sulfate proteoglycans are essential components of the unconventional export machinery of FGF-2. *Proc. Natl. Acad. Sci. U.S.A.* **103,** 15479–15484